ORIGINAL PAPER-EXPLORATION GEOLOGY

Geochemical characteristics and oil–oil correlation of the upper Cretaceous oils from the Iranian part of the Persian Gulf Basin

Faramarz Talaie[1] · Ali Kadkhodaie[2] · Mehran Arian[1] · Mohsen Aleali[1]

Abstract

The Cenomanian Sarvak oil reservoirs are distributed over large areas of the Persian Gulf basin. The purpose of this study is analyzing the geochemical characteristics of the Sarvak oil reservoirs and their inter-relationships in the Persian Gulf, classification of the Sarvak oil samples and investigation of the possible causes of the genetic difference in oil families. In the previous studies, limited samples of Sarvak oil reservoir in scarce oilfields were studied individually and local interpretations are made accordingly. The current study employs a more complete set of geochemical from the Iranian part of Persian Gulf and regional interpretations are drawn. To achieve this goal, the geochemical data of 41 oil samples from 10 oilfields were collected and assessed based on gas chromatography (GC), gas chromatography–mass spectrometry (GC–MS), and stable carbon isotope analysis. It was demonstrated with the evaluations that the oils accumulated in the Upper Cretaceous Sarvak reservoirs in the Persian Gulf basin originate from different source rocks. The oil samples are genetically classified into four oil families based on the similarities and differences of parameters related to the depositional environment-dependent parameters using hierarchical cluster analysis (HCA), star diagram, and stable carbon isotope diagram. The source rocks were mainly deposited in anoxic marine carbonate environments. The thermal maturity of the oils was evaluated using steranes and trisnorhopanes. Oil families 2 and 4 (located at the center of the Persian Gulf) have the highest thermal maturity compared to the other samples; in contrast, oil family 1 (located at the west of the Persian Gulf) has the lowest thermal maturity. The possible source rocks of oil family 1 and family 3 (located at eastern Persian Gulf) using C_{28}/C_{29} steranes are the upper Cretaceous successions; in contrast, the possible source rocks of oil families 2 and 4 are the upper Triassic and Lower Jurassic formations. Results of the study show a high similarity between the oils of families 2 and 4, which are located at the center of the Persian Gulf; these results also recognize the significant difference between these two oil families and oil families 1 and 3. The significant issue raised in this study is to find out the reason for this difference. The structural analysis of the central Persian Gulf shows that huge vertical faults created by salt domes intrusion provided the migration pathways for trapping oil in Sarvak reservoirs. The oils of the Surmeh, Fahliyan, and Dariyan reservoirs have migrated upwards through these faults to be trapped in the Sarvak Formation across the central Persian Gulf.

Keywords Sarvak reservoir · Oil–oil correlation · Depositional environment · Thermal maturity · Source rock age · Hierarchical cluster analysis · Geochemical analysis

Abbreviations

Asph	Asphaltene
Aro	Aromatic
DBT	Dibenzothiophene
Dia	Diasterane
EOM	Extractable organic matter

✉ Ali Kadkhodaie
kadkhodaie_ali@tabrizu.ac.ir

Faramarz Talaie
faramarztalaie@yahoo.com

Mehran Arian
mehranarian@srbiau.ac.ir

Mohsen Aleali
m.aleali@srbiau.ac.ir

1 Department of Earth Sciences, Science and Research Branch, Islamic Azad University, Tehran, Iran

2 Earth Sciences Department, Faculty of Natural Sciences, University of Tabriz, Tabriz, Iran

Gam   Gammacerane biomarker ($C_{30}H_{52}$)
GC   Gas Chromatography
GC–MS   Gas Chromatography–Mass Spectrometry
HCA   Hierarchical cluster analysis
IOOC   Iranian Offshore Oil Company
Mor   Moretanes (C_{31} Mor)
P   Phenanthrene
PDB   Pee Dee Belemnite
Phy   Phytane
Pr   Pristane
Pr/Phy   Pristane to Phytane ratio
Reg   Regular Sterane
Res   Resin
Sat   Saturate
TA   Triaromatic
Tm   C27 17α-22,29,30-trisnorhopane
Ts   C27 18α-22,29,30-trisnorneohopane

Introduction

The Persian Gulf basin and the surrounding coastal areas comprise about 60% of the world's crude oil reserves and 40% of the world's gas reserves (Alsharhan 2014; Baniasad et al. 2021). The tectonic features and the presence of geological structures, as well as the presence of layers rich in organic matter, thick carbonates of porous and permeable layers and the placement of extensive shaly and seal evaporite beds on them, have led to the formation of such huge hydrocarbon reserves (Pollastro 2003; Bordenave and Hegre 2010). The Sarvak Formation together with the Asmari Formation are the host for the largest crude oil reserves in this region. Formerly, various geochemical studies have been conducted in the Persian Gulf region. Rabbani et al. (2014) classified 33 oil samples from different reservoirs of the Persian Gulf region into four oil families based on principal data and biomarker review, which are given as follows: Oil family 1 includes the Jurassic to Lower Cretaceous oil reservoirs in the Doroud, Abouzar, Kharg, and Forouzan oilfields in the northwest of the Persian Gulf region that originated from the Jurassic source rocks and formed in an anoxic marine environment, oil family 2 includes the Jurassic to Lower Cretaceous oil reservoirs in the Balal, Reshadat, Resalat, and Salman oilfields in the central Persian Gulf that originated from the Jurassic source rocks and formed in the dysoxic to oxic depositional environment, oil family 3 includes the Cretaceous to Tertiary oil reservoirs in the Soroosh, Nowrooz, Doroud, Abouzar, Kharg, and Bahregansar in the northwest of the Persian Gulf that likely originated from the Cretaceous source rocks, and oil family 4 is the upper Cretaceous oil reservoirs in the Sirri E, Sirri D, Sirri C, Sirri A, Reshadat and Resalat oilfields in the east of the Persian Gulf that probably originated from the middle Cretaceous source

rocks. Alizadeh et al. (2017) studied the oil samples from the Jurassic to Cretaceous reservoirs. They divided the samples into two oil families. Oil family 1 includes the Jurassic oil reservoirs in the west of the Persian Gulf, and oil family 2 represents the Cretaceous oil reservoirs in the east of the Persian Gulf. Mashhadi and Rabbani (2015) collected six samples from the Sarvak reservoirs and thirteen samples from the other reservoirs in the east of the Persian Gulf. They presented two separate oil families. The five samples of the Sarvak reservoirs fall into oil family one indicating their sources are probably the Ahmadi member, the Gurpi, and Kazhdumi Formation. The noteworthy point in these studies is that the samples have been selected from reservoirs belonging to different periods. Therefore, the oil–oil correlation has not been studied specifically in the Cenomanian Sarvak oil reservoirs in the Persian Gulf. The Sarvak Formation was not continuously expanded on the Persian Gulf and has a gap in the region between the center and west of the Persian Gulf (Rabbani 2013). Due to the discontinuous expansion of the Sarvak Formation and the existence of structural features such as giant salt domes, folds, and faults, it is essential to investigate the continuity of the Sarvak reservoirs and the oil–oil correlation. Considering that this issue has not been investigated yet, in this study, we are looking for the answer. Therefore, if the oils are not compatible and the reservoirs are not linked, its cause should be investigated in the future studies and the source of the oils should be determined. The oil–oil correlation method has been applied to identify petroleum systems and reservoir compartments, which increase productivity and reduce exploration and production costs. In this study, the Sarvak oil reservoirs in the Persian Gulf are grouped and their origin is discussed. Also, the reason for the genetic similarity of the oils from the Sarvak reservoirs with the older reservoirs including the Dariyan, Fahliyan, and Surmeh in the central part of the Persian Gulf has been determined by using the evaluation of possible factors. One of the main applications of the present study is to identify the oil fields in the Persian Gulf basin, in which their Sarvak oil reservoirs are linked or have an oil of the same origin. Accordingly, it is possible to predict the location of future wells and increase production by the geochemical model of these fields.

Geological setting

The Persian Gulf sedimentary basin is located in the eastern part of the Arabian Shield, where the Arabian plate subducts beneath the Eurasian plate. This basin is restricted in the north and east by the folded Zagros region and in the west and south by the Arab shield. In addition to the Persian Gulf, this region includes the Oman Sea and the sedimentary basin of the Zagros orogeny foredeep (Konyuhov and

Maleki 2006). The sequence of the sedimentary layers in the offshore Persian Gulf and onshore Zagros folded zone developed from the Precambrian to Quaternary (Ghazban 2007). The Persian Gulf basin comprises a Miocene-Recent sedimentary basin that was formed in reaction to a continuous collision between the Arabian shield and the Eurasian plate (Sepehr and Cosgrove 2004; Hessami et al. 2006; Allen and Armstrong 2008).

The relationship between sedimentary basins (e.g. Khavari et al. 2009; Arian et al. 2012; Arian and Aram 2014; Ehsani and Arian 2015; Aram and Arian 2016; Kadkhodaie and Kadkhodaie 2022a, b) and basement faulting (e.g. Arian 2012; Nouri et al. 2013; Nouri and Arian 2017; Nabilou et al. 2018; Mansouri et al. 2017, 2018) indicates the role of faults in the control of sedimentary basins in Iran. In terms of lithofacies, especially the role of tectonics, the Iran sedimentary basin is divided into several large tectonic-stratigraphic units (Arian 2015; Razaghian et al. 2018; Taesiri et al. 2020). In the study area, the Persian Gulf as a peripheral foreland basin has been affected by blind faults and their branches. They have been formed and developed by the Arabian–Eurasian plate convergency.

Within Albian-Cenomanian, the Persian Gulf region has been recognized by extensive intrashelf basins in shallow-water carbonate platforms. The Sarvak Formation was formed on a carbonate platform during the Albian to Turonian age and developed along the Zagros, Dezful embayment, and Persian Gulf basin. (James and Wynd 1965; Motiei 1993).

The sediments of the formation in the type section (Tang-e Sarvak) reach a thickness of about 822 m and consist of two main facies: first, a massive limestone of the shallow-water environment (neritic zone), including euphotic macrofauna (such as *algae*, *rudist*, *gastropods*, *pelecypods*) and benthic foraminifera, and the second facies is the thin-bedding argillaceous limestone from deeper marine characterized by pelagic fauna (*Oligostegina*, *Globigerina*, etc.) (Motiei 1993). The contact of the Sarvak Formation with the upper part of Kazhdumi shales is gradational. In contrast, the upper border of this formation with the Gurpi Formation is clear and accompanied by an erosion zone in the type section (Tang-e Sarvak). In the Persian Gulf and Coastal Fars, the Laffan Shale separates the Ilam and Sarvak formations with characteristic peaks in Gamma logs.

In the study area, the Sarvak Formation is divided into the Mishrif, Mauddud and Ahmadi members (Fig. 1). These members are comparable and named from Mishrif, Ahmadi, and Mauddud formations in Iraq (Owen and Nasr 1958). The name "Mishrif member" referred to the limestone observed below the unconformity between the Sarvak formation and the Laffan shale. The Mishrif member is composed of micritic, skeletal, and reefal argillaceous limestone with interbedded marl and shale. This member has diverse components in different sections including rudist reef complex, coral, rudist bioherms, rare planktonic, and benthic foraminifera (El-Naggar and Al-Rifai 1972). In the study area, the reservoir zone is the upper part of the Sarvak Formation (Mishrif member).

Materials and methods

A total of 41 samples from the 10 oilfields in the west, central and east of the Persian Gulf basin were collected (Fig. 2) and studied based on geochemical experiments. First, the oil samples were decomposed into different hydrocarbon fractions by liquid chromatography. The main part of liquid column chromatography is the stationary phase, which is composed of solid material with the property of absorbing fluids. The adsorbent solids in this study are silica and alumina powders. Oil and extractable organic matter (EOM) were separated into hydrocarbons and non-hydrocarbon such as saturate, aromatic and resins fractions. The saturated, aromatic, and resin fractions were, respectively, dissolved by n-hexane, benzene, and methanol solvent (Baniasad et al. 2016). The excess of each solvent is removed from the sample using a rotary evaporator.

The n-alkalkanes, pristanes and phytanes in the oil composition were measured by the Varian-CP-3800 gas chromatography with 5 CB CP-Sil capillary columns (25 μm × 25 m) (Fig. 3). The GC analysis was performed at the Research Institute of Petroleum Industry (RIPI Lab) (Table 1).

Gas chromatography with mass spectrometry (GC–MS) is applied for the analysis of biological markers that have been used in correlation studies and in the assessment of the thermal maturity of the oils and extracts. The biological markers which are primarily used in this study are steranes and triterpanes (Table 2). The main sources of steranes and triterpenes are sterols in the cell membrane of organisms including higher plants and algae (overview in Mackenzie et al., 1983). The steroids or sterols during diagenesis and catagenesis are degraded and turn into steranes and triterpanes. The hopanes are triterpene compounds (pentacyclic), and they are classified as aliphatic hydrocarbons. The source of this compound in living organisms is the membrane component of prokaryotic cells such as phototrophic cyanobacteria and heterotrophic bacteria (Ourisson et al. 1987).

The mixture to be analyzed is injected with an injection chamber into the Agilent 7890-A gas chromatograph with an Agilent 7883-B automatic sampling (available in AGH University of Science and Technology), where the various compounds are separated according to the speed at which they move through the gas chromatographic column contains molten silica capillary (60 m × 0.25 mm id) with 95% Methyl/5% Phenylsilicone phase (Baniasad et al. 2016).

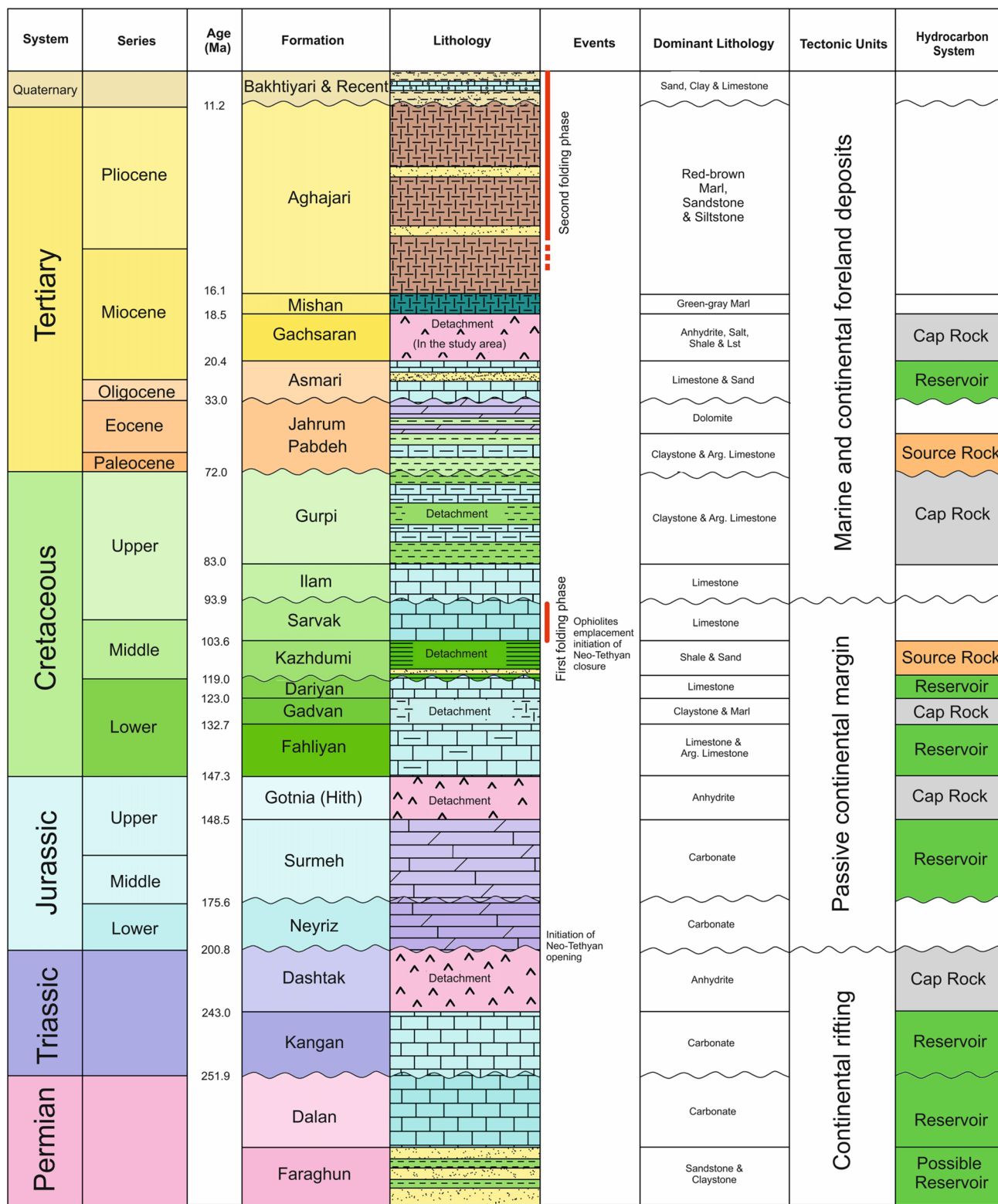| System	Series	Age (Ma)	Formation	Lithology	Events	Dominant Lithology	Tectonic Units	Hydrocarbon System
Quaternary		11.2	Bakhtiyari & Recent			Sand, Clay & Limestone		
Tertiary	Pliocene		Aghajari		Second folding phase	Red-brown Marl, Sandstone & Siltstone	Marine and continental foreland deposits	
	Miocene	16.1 / 18.5	Mishan			Green-gray Marl		
		20.4	Gachsaran	Detachment (In the study area)		Anhydrite, Salt, Shale & Lst		Cap Rock
	Oligocene	33.0	Asmari			Limestone & Sand		Reservoir
	Eocene		Jahrum			Dolomite		
	Paleocene	72.0	Pabdeh			Claystone & Arg. Limestone		Source Rock
Cretaceous	Upper	83.0	Gurpi	Detachment		Claystone & Arg. Limestone		Cap Rock
		93.9	Ilam		First folding phase	Limestone		
	Middle	103.6	Sarvak		Ophiolites emplacement initiation of Neo-Tethyan closure	Limestone	Passive continental margin	
		119.0	Kazhdumi	Detachment		Shale & Sand		Source Rock
	Lower	123.0	Dariyan			Limestone		Reservoir
		132.7	Gadvan	Detachment		Claystone & Marl		Cap Rock
		147.3	Fahliyan			Limestone & Arg. Limestone		Reservoir
Jurassic	Upper	148.5	Gotnia (Hith)	Detachment		Anhydrite		Cap Rock
	Middle		Surmeh			Carbonate		Reservoir
	Lower	175.6	Neyriz		Initiation of Neo-Tethyan opening	Carbonate		
Triassic		200.8	Dashtak	Detachment		Anhydrite	Continental rifting	Cap Rock
		243.0	Kangan			Carbonate		Reservoir
Permian		251.9	Dalan			Carbonate		Reservoir
			Faraghun			Sandstone & Claystone		Possible Reservoir

Fig. 1 The Permian-Quaternary lithostratigraphic column in the Persian Gulf was modified after Ghanadian et al. (2017) and Mohammadrezaei et al. (2020)

Fig. 2 The map of the oilfields and gas accumulations in the Persian Gulf (the studied oilfields are shown with red color) (After Alsharhan 2014)

The compounds are carried with Helium. The decomposed sections of hydrocarbons come out of the chromatographic column and arrive at the ion chamber, respectively. At this stage, the separated compounds lose electrons and become + 1 ions. These components are then separated from each other using a magnetic field due to the difference in mass-to-charge ratio (m/z). Finally, the amount of separated ions is measured by the detector. The values of the stable carbon isotope of hydrocarbons fraction were calculated by the mass spectrometer Finnigan Delta Plus device with the standard of Pee Dee Belemnite (PDB) and ± 0.2 ‰ accuracies (Table 1) (Baniasad et al. 2016).

Results and discussion

Oil–oil correlation

One of the problems in using geochemical parameters to analyze oil–oil correlation is the identification of factors affecting the biomarkers including thermal maturity, type of organic matter or microbial degradation. The 20S/(20S + 20R) steranes ratio is sensitive to thermal maturity, the C_{27}, C_{28}, C_{29} regular steranes are affected by the type of organic matter and some other parameters such as Dia/
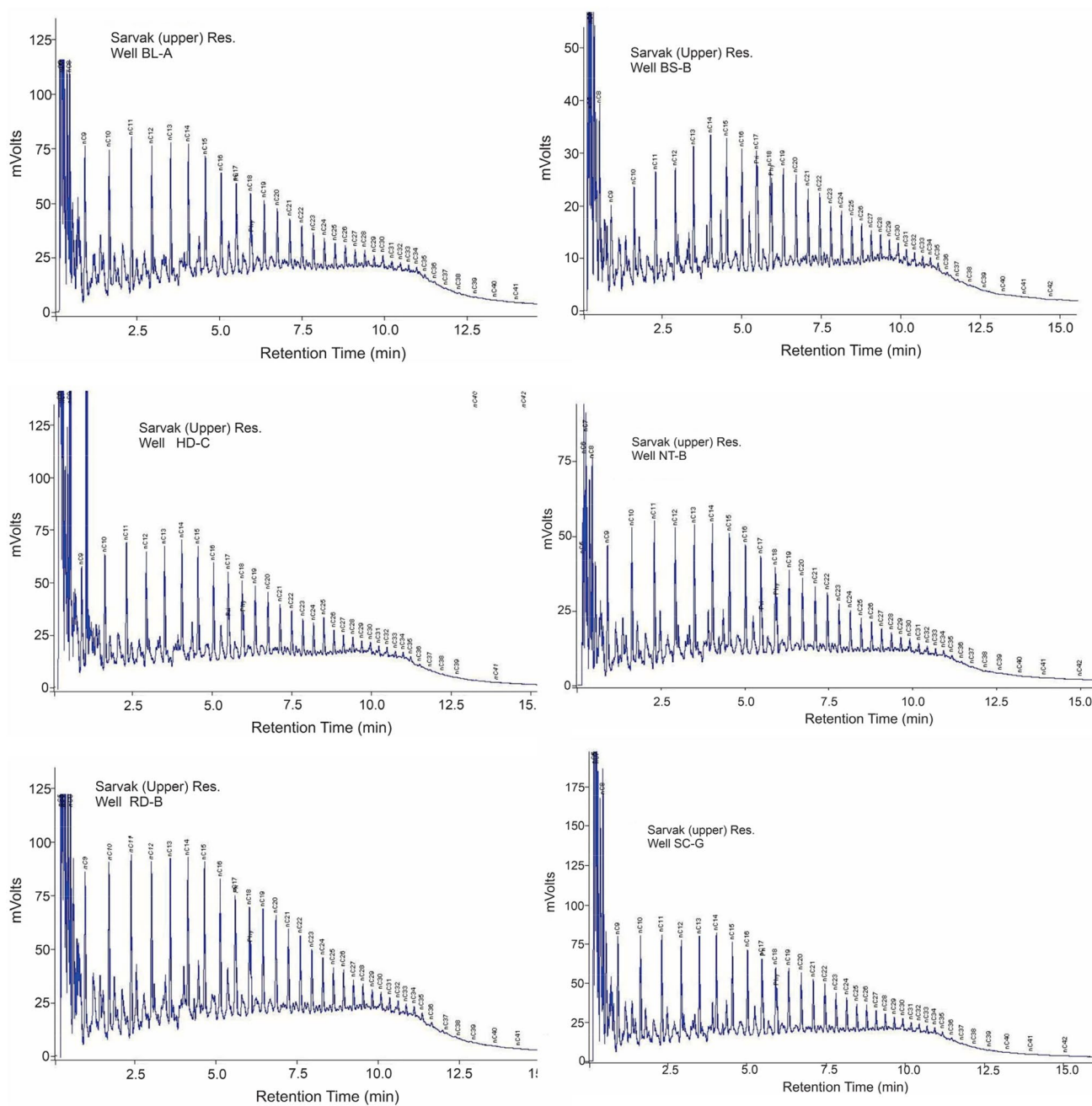
Fig. 3 Gas chromatography (GC) diagram of six selected oil samples showing the abundances of n-alkanes, pristane and phytane

(Dia + Reg) steranes and Ts/(Ts + Tm) are affected by the thermal maturity and the sedimentary environment's conditions. Therefore, in this study, different parameters were employed for oil–oil correlation. The biomarker parameters are usually more important than the bulk parameters of the oil in the process of determining the oil–oil correlation (Peters et al. 2005). Because they are more resistant to diagenetic processes and have more accurate genetic information about the origin of the oil.

Statistical study

Hierarchical cluster analysis (HCA) is one of the statistical methods to examine the similarities and differences in the characteristics of the oil samples. In this method, the distance between variables in the statistical population is enumerated and compared with each other. Thus, the relationship of the samples is determined using a dendrogram (Ward 1963). Then, the samples are grouped, if

Table 1 GC analysis and the stable carbon isotope of the Sarvak, Dariyan, Fahliyan, and Surmeh oil samples

Sample ID	Pri/Phy	Pri/nC$_{17}$	Phy/nC$_{18}$	δ13C Sat (‰)	δ13C Oil (‰)	δ13C Aro (‰)	δ13C Res (‰)	δ13C Asph (‰)
BL-A	0.45	NA	NA	−27.39	−27.10	-27.08	NA	NA
BL-B	0.92	NA	NA	−27.66	−27.50	−27.04	NA	NA
BL-S1	0.94	0.32	0.38	−27.39	−27.14	−27.08	−27.17	−27.16
BL-S2	0.61	0.25	0.44	−27.66	−27.48	−27.04	−27.14	−27.47
HD-A	1.02	0.76	0.77	−27.44	−26.42	−26.71	−26.26	−26.27
HD-B	1.01	0.76	0.76	−27.16	−26.23	−26.33	−26.15	−25.80
HD-C	0.79	0.31	0.41	−27.60	−27.50	−27.40	−27.20	−27.50
BS-A	1.02	0.79	0.82	−27.14	−26.10	−26.53	−25.80	−25.52
BS-B	0.59	0.37	0.72	−28.30	−27.60	−27.30	−27.10	−27.20
SC-E	0.09	0.03	0.56	−27.40	−26.60	−26.20	−25.90	−26.20
SC-F	1.20	0.57	0.54	−27.30	−26.60	−26.20	−26.20	−26.50
SC-G	0.28	0.12	0.61	−27.00	−26.80	−26.40	−26.00	−26.60
SD-B	0.58	0.26	0.53	−27.10	−26.70	−26.30	−26.00	−26.50
SD-C	0.37	0.16	0.54	−27.20	−26.40	−26.10	−26.40	−26.60
SD-A	NA	NA	NA	−27.20	−26.60	−26.40	−26.10	−26.40
SD-D	1.02	0.52	0.55	−27.30	−26.70	−26.30	−25.90	−26.50
SE-A	NA	NA	NA	−27.20	−26.50	−26.20	−25.70	−26.10
SE-B	0.34	0.13	0.52	−27.10	−26.50	−26.00	−25.80	−26.20
SE-C	0.70	0.32	0.55	−27.10	−26.60	−26.40	−26.00	−26.50
SE-D	0.74	0.32	0.55	−27.10	−26.60	−26.50	−26.30	−25.70
SE-E	0.37	0.14	0.52	−27.40	−26.70	−26.10	−26.20	−26.50
SE-F	1.20	0.52	0.51	−27.30	−26.50	−26.00	−26.10	−26.20
RE-A	0.97	0.42	0.52	−27.00	−26.60	−26.40	−26.10	−26.50
RE-B	NA	NA	NA	−27.10	−26.50	−25.80	−26.10	−26.50
RE-D1	0.86	0.45	0.56	NA	NA	NA	NA	NA
RE-D2	0.70	0.24	0.38	NA	NA	NA	NA	NA
RE-S1	0.70	0.24	0.38	NA	NA	NA	NA	NA
RE-S2	0.89	0.31	0.39	−27.19	−26.88	−26.63	−26.19	−26.97
NT-A	0.87	0.45	0.54	−27.30	−26.60	−26.10	−25.90	−26.40
NT-B	0.81	0.41	0.57	−26.90	−26.60	−26.30	−25.90	−26.40
NT-C	NA	NA	NA	NA	NA	NA	NA	NA
NT-D	NA	NA	NA	−27.10	−26.70	−26.50	NA	NA
RD-A	NA	NA	NA	−26.80	−26.50	−25.80	−26.40	−26.70
RD-B	0.46	NA	NA	−27.10	−26.80	−26.60	−26.60	−26.20
RD-D	0.91	0.29	0.36	−27.55	−26.94	−26.90	−27.11	−27.09
SL-F1	0.58	0.24	0.46	NA	NA	NA	NA	NA
SL-F2	0.59	0.17	0.36	NA	NA	NA	NA	NA
SL-S1	0.87	0.47	0.64	NA	NA	NA	NA	NA
SL-S2	0.80	0.29	0.40	−27.33	−27.03	−26.81	−26.72	−26.50
SL-S3	0.78	0.26	0.38	−26.98	−26.70	−26.71	−26.42	−26.55
SL-S4	0.88	0.33	0.40	−27.31	−26.89	−26.66	−26.72	−26.70

the parameter values have affinities. The HCA statistical study was performed using MATLAB software based on 22 geochemical parameters. Since the oils are classified based on the origin and type of organic matter, the biomarker parameters that are sensitive to thermal maturation were not used. According to this diagram, the oils of the Sarvak reservoirs in the Iranian part of the Persian Gulf are divided into four oil families (Fig. 4).

Oil family 1 includes the oils of the Bahregansar and Hendijan oilfields in the west of the Persian Gulf region. Oil family 2 includes the RD-A, RE-A, NT-C, HD-C, and BL-A samples from the Reshadat, Resalat, Nosrat, Hendijan

Table 2 The GC–MS analysis data of the Sarvak, Dariyan, Fahliyan, and Surmeh oil samples

Sample ID	C22t/C21t	C19t/C23t	Mor/C30H	C24Tet/C23t	C29H/C30H	C30DiaH/C30H	C26t/C25t	Gam/C31HR	Steranes/Terpanes	C35HS/C34HS	Ts/(Ts+Tm)	C27Dia/(Dia+Reg)	C29 ααα 20S/(S+R)	DBT/P
BL-A	0.65	0.25	0.08	1.85	0.95	0.05	0.47	0.14	0.15	0.14	0.49	0.47	0.43	2.33
BL-B	0.75	0.30	0.09	NA	NA	NA	NA	0.10	NA	1.04	NA	NA	0.53	NA
BL-S1	0.34	0.86	0.08	2.55	0.98	0.12	0.63	0.53	0.3	0.64	0.77	0.76	0.43	2.35
BL-S2	0.39	0.78	0.07	2.51	1.07	0.15	0.53	0.19	0.3	0.63	0.77	0.75	0.43	2.26
HD-A	0.69	0.08	0.06	0.41	0.87	0.12	0.7	0.16	0.23	1.2	0.32	0.38	0.47	0.60
HD-B	0.93	0.03	0.06	0.21	1.1	0.02	0.78	0.17	0.15	1.33	0.24	0.23	0.45	0.79
HD-C	0.58	0.26	0.11	1.32	1	0.03	0.63	0.37	0.29	0.85	0.34	0.36	0.48	0.98
BS-A	0.29	0.1	0.05	0.42	0.57	0.06	0.76	0.16	0.28	0.97	0.56	0.63	0.51	0.34
BS-B	0.38	0.08	0.08	0.72	0.57	0.04	0.51	0.3	0.38	1.03	0.40	0.54	0.52	0.90
SC-E	0.58	0.06	0.06	0.48	0.73	0.02	0.6	0.25	0.26	1.29	0.31	0.38	0.48	1.88
SC-F	0.51	0.09	0.07	0.66	0.86	0.02	0.43	0.27	0.25	1.17	0.31	0.38	0.47	1.57
SC-G	0.72	0.08	0.08	0.45	0.77	0.02	0.57	0.2	0.25	0.9	0.30	0.38	0.45	1.90
SD-A	0.64	0.06	0.06	0.29	0.95	0.02	0.82	0.16	0.17	1.17	0.29	0.48	0.50	1.77
SD-B	0.54	0.14	0.09	0.53	0.85	0.02	0.24	0.15	0.3	0.92	0.29	0.34	0.50	1.57
SD-C	0.49	0.1	0.08	0.51	0.84	0.02	0.14	0.25	0.29	1.17	0.28	0.34	0.44	0.83
SD-D	0.67	0.07	0.08	0.51	0.76	0.02	0.54	0.22	0.27	0.95	0.30	0.41	0.50	1.78
SE-A	0.51	0.09	0.06	0.41	0.84	0.02	0.91	0.16	0.16	1.17	0.34	0.40	0.42	1.40
SE-B	0.5	0.17	0.13	0.62	0.68	0.03	0.18	0.32	0.29	0.9	0.33	0.47	0.51	1.62
SE-C	0.42	0.14	0.07	0.63	0.78	0.02	0.23	0.25	0.27	1.18	0.31	0.44	0.49	1.27
SE-D	0.42	0.14	0.08	0.59	0.85	0.02	0.35	0.25	0.25	1.14	0.31	0.42	0.47	1.08
SE-E	0.48	0.1	0.08	0.67	0.85	0.02	0.39	0.25	0.21	1.28	0.30	0.36	0.47	1.38
SE-F	0.49	0.1	0.08	0.67	0.79	0.02	0.38	0.28	0.23	1.27	0.30	0.35	0.49	1.53
RE-A	0.57	0.56	0.05	1.87	1.02	0.06	0.88	0.05	0.25	0.85	0.63	0.71	0.44	1.19
RE-B	0.97	0.04	0.08	NA	NA	NA	NA	0.14	NA	1.03	NA	NA	0.53	NA
RE-D1	1.08	0.04	0.07	0.36	1.11	0	0.4	0.32	0.21	1.35	0.22	0.25	0.47	1.5
RE-D2	1	0.37	0.08	2.01	1.2	0.09	0.69	0.22	0.11	0.97	0.7	0.28	0.34	3.16
RE-S1	0.56	0.59	0.13	2	0.79	0.04	0.83	0.13	0.24	0.63	0.53	0.66	0.45	2.23
RE-S2	0.8	0.47	0.08	2.07	0.92	0.03	0.44	0.29	0.18	0.97	0.5	0.59	0.48	2.56
NT-A	0.67	0.07	0.07	0.52	0.91	0.02	0.44	0.26	0.21	1.27	0.28	0.32	0.46	1.72
NT-B	0.87	0.07	0.08	0.37	0.96	0.02	0.58	0.24	0.22	0.96	0.27	0.38	0.50	2.08
NT-C	0.65	0.6	0.06	1.99	1.01	0.05	0.87	0.09	0.15	0.98	0.61	0.67	0.44	1.54
NT-D	0.57	0.09	0.08	NA	NA	NA	NA	0.08	NA	0.86	NA	NA	0.50	NA
RD-A	0.68	0.56	0.04	1.84	1.01	0.06	0.86	0.08	0.16	0.86	0.62	0.69	0.46	1.40
RD-B	0.57	0.08	0.07	0.59	0.95	0.02	0.43	0.29	0.25	0.91	0.32	0.38	0.47	0.73

Table 2 (continued)

Sample ID	C22t/C21t	C19t/C23t	Mor/C30H	C24Tet/C23t	C29H/C30H	C30DiaH/C30H	C26t/C25t	Gam/C31HR	Steranes/Terpanes	C35HS/C34HS	Ts/(Ts+Tm)	C27Dia/(Dia+Reg)	C29 αααα 20S/(S+R)	DBT/P
RD-D	0.56	0.53	0.08	2.3	0.98	0.04	0.36	0.33	0.2	1.08	0.59	0.62	0.43	2.03
SL-F1	0.72	0.34	0.08	2	1.06	0.03	0.41	0.09	0.16	1.02	0.47	0.52	0.48	2.45
SL-F2	0.6	0.55	0.08	2.17	0.92	0.06	0.51	0.13	0.26	0.94	0.6	0.63	0.47	2.47
SL-S1	0.9	0.12	0.08	1.47	0.9	0.04	0.39	0.2	0.17	0.48	0.49	0.58	0.44	0.61
SL-S2	0.8	0.33	0.08	1.89	1.03	0.03	0.46	0.12	0.17	0.99	0.47	0.54	0.48	2.35
SL-S3	0.82	0.35	0.07	1.43	1	0.03	0.42	0.15	0.23	1	0.47	0.61	0.51	2.59
SL-S4	0.64	0.45	0.07	2.21	1.02	0.05	0.5	0.28	0.21	0.97	0.55	0.58	0.48	2.48

and Balal oilfields that with the exception of Hendijan, the rest of the oilfields are located in the center of the Persian Gulf. Oil family 3 comprises all samples of the Sirri E, Sirri D, Sirri C, and NT-A and NT-B samples from the Nosrat oilfield and RE-B sample from the Resalat oilfield. Oil family 4 includes the oils of the Surmeh, Shuaiba, Fahliyan and Dariyan reservoirs belonging to the Resalat, Reshadat and Salman oilfields.

The star diagram of the samples is plotted using 11 parameters that depend on the sedimentary environment and the type of organic matter. This diagram is a reliable tool for evaluating the oil–oil correlation. As is seen, star diagrams confirm the classification conducted by the HCA method. In the star diagram of oil family 2, a good correlation can be seen between the samples. In addition, the difference in the origin of the samples of oil family 2 with oil families 1 and 3 is quite apparent (Fig. 5). Due to the high similarity between oil families 2 and 4 and also the genetic differences between oil families 1 and 3, the relationship between the oil families 2 and 4 is an issue that needs to be investigated. The variation in the number of stable carbon isotopes in hydrocarbon fractions depends on the sedimentary environment conditions. Therefore, the stable carbon isotope diagram is an applied method for comparing the genetic similarity and differences in crude oils (Galimov 1973). The trend of stable carbon isotope values of the hydrocarbon fractions in the Galimov diagram suggests the similarity of oil families (Fig. 5).

Depositional environment

The amount of pristane and phytane molecules in the oil composition is one of the most important detectors of the redox conditions in the paleoenvironment. The process of converting the phytyl chain from biological organisms (bacteriochlorophylls sulfur bacteria) to phytol and then phytan takes place in marine/lacustrine anoxic environments, in sedimentary environments with oxic water, the phytyl is oxidized and produces phytenic acid. Phytenic acid is converted to pristene and then to pristine (Powell and McKirdy 1973; Peters et al. 2005). Due to this issue, the value of the Pr/Ph ratio in the oil composition is directly related to the Eh of the depositional environment and inversely related to its pH. The oils generated from the reducing depositional environment have Pr/Ph ratio values less than one and the oils generated from the oxic depositional environment have Pr/Ph values greater than three (Didyk et al. 1978). Also, values of this ratio between 1 and 3 indicate that the oil sources are dysoxic depositional environments. The values of this ratio in the oil samples are between 0.09 and 1.2. Thus, the oils of the Sarvak reservoirs in this region originated from the source rocks that formed in the anoxic marine depositional environment

Fig. 4 Hierarchical cluster analysis (HCA) of the studied oil samples. The samples are classified into four families based on 22 geochemical parameters
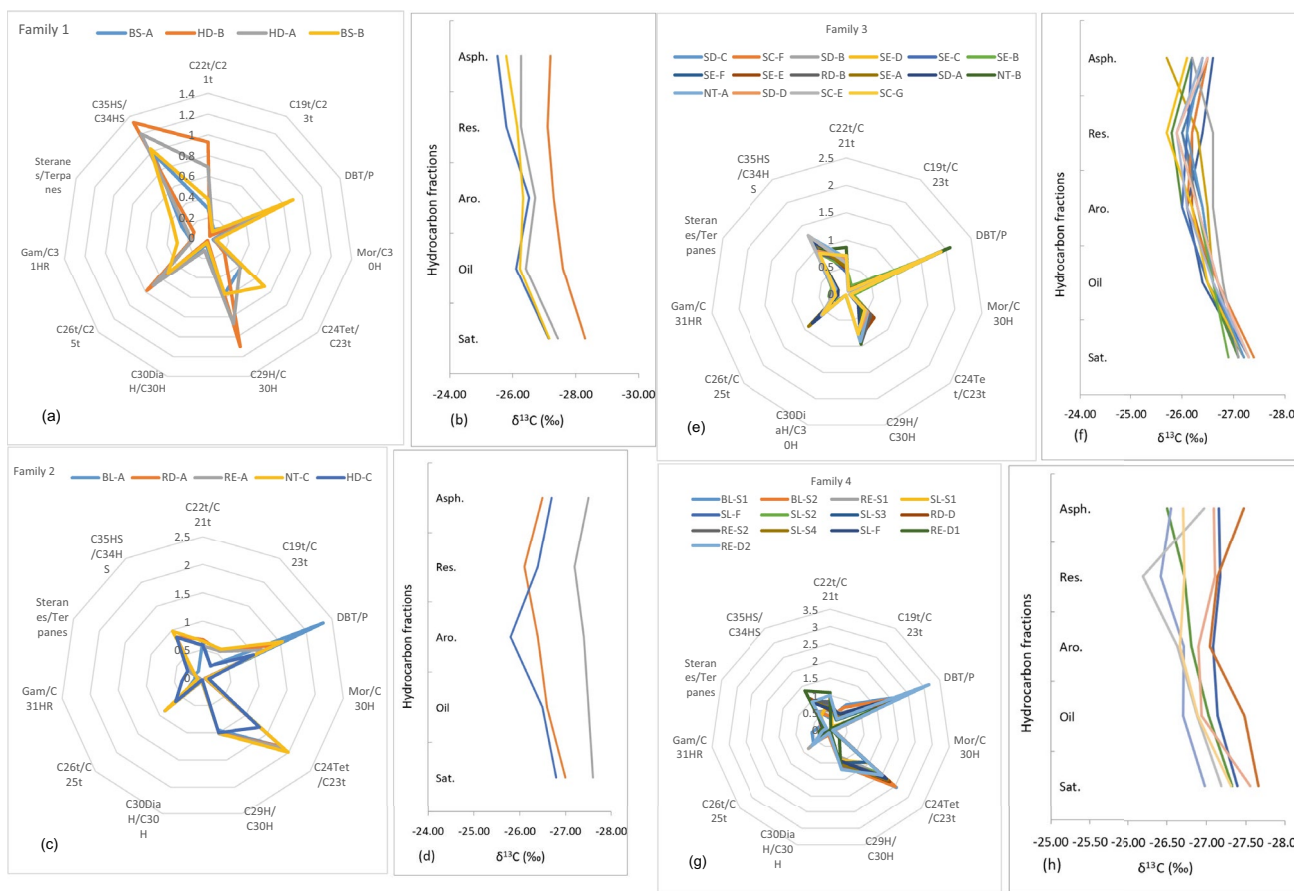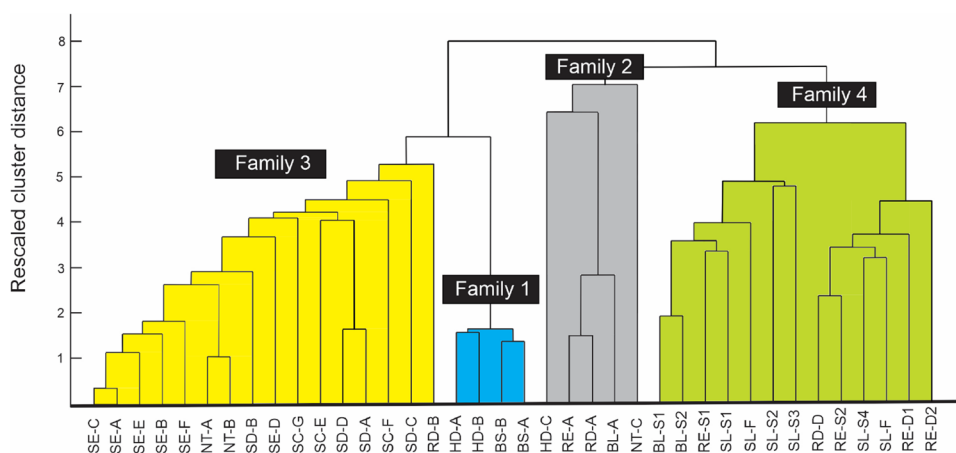

Fig. 5 Star diagrams of oil families based on 11 parameters relevant to the depositional environment and stable carbon isotope diagram of hydrocarbon fractions. Both diagrams confirm the good correlation of oil samples belonging to each family. The genetic similarity of the oil family 2 and 4 is also illustrated. **a** Star diagram of oil family 1. **b** stable carbon isotope diagram of oil family 1. **c** Star diagram of oil family 2. **d** stable carbon isotope diagram of oil family 2. **e** Star diagram of oil family 3. **f** stable carbon isotope diagram of oil family 3. **g** Star diagram of oil family 4. **h** stable carbon isotope diagram of oil family 4

with low Eh and high pH to marine depositional environments with moderate Eh and pH. As is seen in Fig. 6, the depositional environments of the source rocks of all samples are in the range of reducing marine environments. In

addition, it is found that the reducing conditions of the sedimentary environment of the source rocks is in the range of anoxic belonging to oil family 3 to dysoxic conditions belonging to oil family 1. The high salinity of water
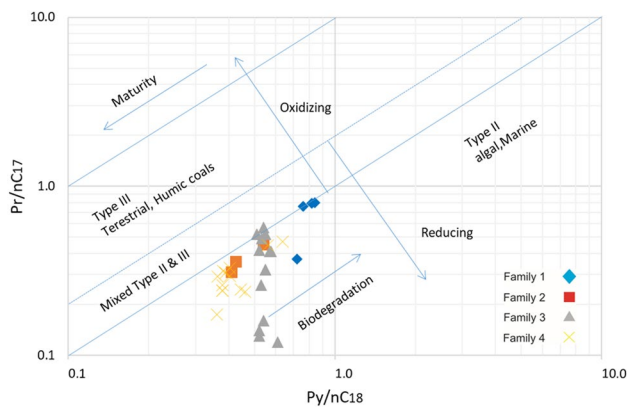
Fig. 6 The plot of Pr/n-C_{17} versus ph/n-C_{18} indicating the depositional environment conditions of source rocks
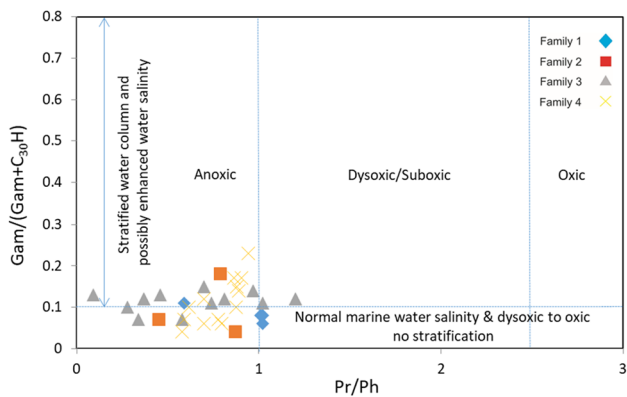
Fig. 7 The plot of Gamm index versus Pr/Ph to assess water column stratigraphy and salinity of the source rocks depositional environment

in the depositional environments of the source rocks is one of the reasons for the high amount of Gammaceranes in the composition of the crude oils (Sinninghe Damsté et al. 1995). Therefore, the Gammacerane index is one of the indicators for the depositional environments' water salinity. In the oils produced from marine environments with normal salinity, the Gammacerane index is less than 0.1, and it is between 0.1 and 0.2 in the oils produced from the low-salinity marine environments (Song et al. 2017).

The Gammacerane index values in the mentioned samples are from 0.04 to 0.18, which indicates the source rocks deposited in the marine environments with normal to low salinity. Using the plot of the Gamm index versus Pr/Ph, the salinity and stratification of the depositional environment water column were determined (Fig. 7).

Accordingly, the samples of oil family 1 are generated from a non-stratification depositional environment with normal salinity. And source rocks of oil families 2, 3 and 4 are formed in the marine environments with low salinity and stratification (Table 3).The Dibenzothiophene and Phenanthrene aromatic biomarkers are used to evaluate the depositional environment and to determine the source rocks facies. The low values of the DBT/P ratio (less than 1) indicate the shale source rocks and high values (greater than 1) show the carbonate source rocks (Hughes et al. 1995). The values of the DBT/P ratio in oil families are variable. In oil family 1, the DBT/P ratio is low falling in the range of 0.34 to 0.9, while in oil families 2, 3 and 4, its values vary from about 1–3.16. As is seen in the plot of DBT/P versus Pr/Ph, the origin of oil family 1 is shale and the combination of shale and carbonate sediments and the origin of oil families 2, 3, and 4 are the carbonate-marl source rocks (Fig. 8).

The ratio of tricyclic terpanes with different carbon atom numbers is a practical parameter for identifying the sedimentary environment of the source rock and the organic matter type (Safaei-Farouji et al. 2022). Usually, the oils derived from the carbonate source rocks have a high C_{22}/C_{21} tricyclic terpanes ratio and a low C_{24}/C_{23} tricyclic terpanes ratio (Peters et al. 2005). Due to this fact, the plot of C_{22}/C_{21} tricyclic terpanes versus C_{24}/C_{23} tricyclic terpanes is used to determine the source rock facies of oil families (Fig. 9). In this diagram, oil families are clearly separated from each other. By observing the results obtained from the depositional environments study, it is concluded that the source rocks of oil family 1 have differences with oil families 2 to 4 in terms of the lithology, type of organic matter, redox conditions, salinity and water column stratification of the depositional environment (Table 3).

Table 3 Summary of geochemical characteristics of oil families

| Properties	Family 1	Family 2	Family 3	Family 4
Redox conditions	Dysoxic	Dysoxic-anoxic	Anoxic	Dysoxic-anoxic
Water salinity and stratification	Normal salinity, without layering	Low salinity and stratification	Low salinity and stratification	Low salinity and stratification
Depositional environment's facies	Shale and shale-carbonate	Carbonate-marl	Carbonate-marl	Carbonate-marl
Thermal maturity	Moderate	High	Low	High
Source rock's age	Cretaceous	Triassic-Jurassic	Cretaceous	Triassic-Jurassic
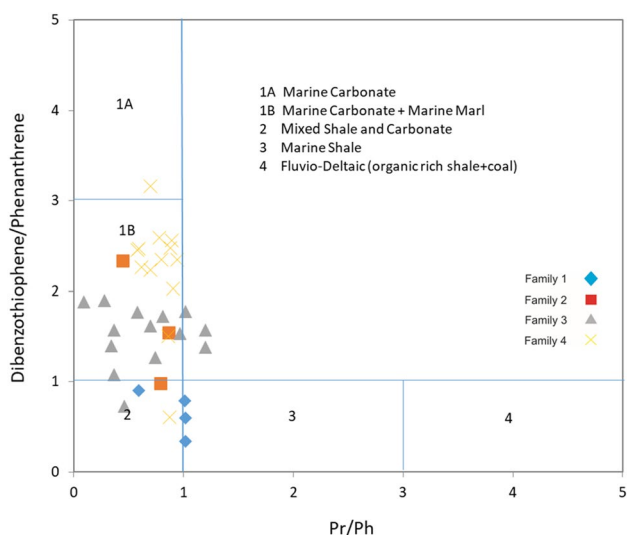
Fig. 8 The plot of DBT/P ratio versus Pr/Ph to determine the source rock facies of oil families
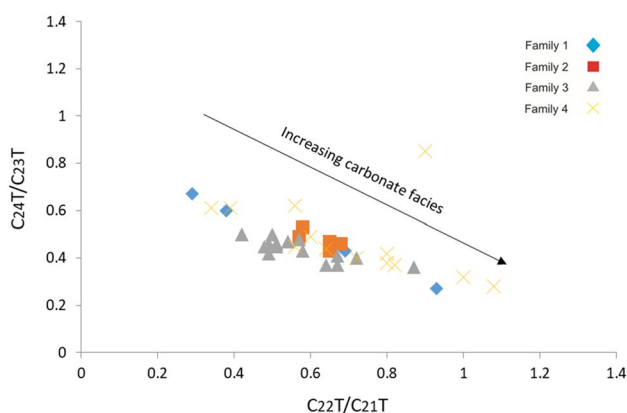

Fig. 9 The diagram of tricyclic terpanes to indicate lithology of oil family's source rocks

Maturity

The biomarkers used to assess thermal maturity are usually also affected by depositional environment conditions and do not provide a precise interpretation of hydrocarbon maturation. Hence, the different parameters of steranes, triterpanes and triaromatic steroids were used to calibrate their results on oil maturity. In the maturation process of complex geopolymers, the molecular structure changes with the increase in temperature and the passing of time (Khalil Khan et al. 2022). Accordingly, the amount of degraded molecules is directly related to the hydrocarbon thermal maturity. The biological composition of the sterol molecule (R side-chain at C-20) is unstable to heat, and it becomes a stable compound (S side-chain at C-20) with increasing

thermal maturity (Mackenzie et al. 1983; Beaumont et al. 1985). This process increases the 20S/(20S + 20R) ratio at C_{29} steranes from 0 to 0.55 during the catagenesis stage (Seifert and Moldowan 1986). The variation of $C_{29}\alpha\alpha\alpha20S/$ (20S + 20R) ratio values in the studied samples is slight in the range from 0.34 to 0.52. The lower resistance of Tm (17α-22,29,30-trisnorhopane) to thermal cracking than Ts (18α-22,29,30- trisnorhopane) decreases the concentration of Tm and increases the concentration of Ts with increasing temperature until the concentration of Tm in the hydrocarbon composition reaches zero at the beginning of the oil generation window (Seifert and Moldowan 1978). In the process of substitution of Tm with Ts, the clay minerals play the role of catalyst (McKirdy et al. 1984). In oils produced from shale source rocks, the Ts/(Ts + Tm) ratio can be increased due to the presence of clay. Therefore, the Ts/ (Ts + Tm) ratio is a useful index for assessing the maturity of oils produced from carbonate source rocks. The values of Ts/(Ts + Tm) ratio in oil family 1 are less than 0.56, in oil family 2 are range from 0.34 to 0.63, in oil family 3 are less than 0.34, and in oil family 4 are in the range of 0.47 to 0.77. Accordingly, oil family 3 located in the east of the Persian Gulf has the lowest thermal maturity and the oil families 2 and 4 located in the center of the Persian Gulf have the highest thermal maturity. The chemical reaction of converting steranes to diasteranes depends on three factors in the depositional environment, including temperature, clay content and pH (Peters et al. 2005). As a result, the diasteranes/ steranes ratio increases with increasing thermal maturity. Also, this ratio is high in hydrocarbons produced from shaly depositional environments (Peters et al. 1990). Therefore, C_{27} Dia/(Dia + Reg) ratio is used along with the $C_{29}\alpha\alpha\alpha20S/$ (20S + 20R) ratio to determine the thermal maturity of oils. The variation of C_{27} Dia/(Dia + Reg) ratio values in the composition of the mentioned oils is almost large and its range is from 0.23 to 0.76. The triaromatic steroids are one of the main biomarkers related to thermal maturity. Therefore, the TA(I)/ TA (I + II) ratio is used as an oil maturity indicator. With increasing temperature, long-chain configurations of triaromatics steroids are degraded to short-chain aromatics due to the sensitivity of this molecule to thermal cracking (Beach et al. 1989). Therefore, thermal maturity is associated with an increase in the TA(I)/TA (I + II) ratio. The total of C_{20} and C_{21} triaromatics are used as TA(I) and the total of C_{20}, C_{21}, C_{26}, C_{27}, C_{28} and C_{29} triaromatics are used as TA(II) (Peters et al. 2005). The variation of this ratio in the samples is large ranging from 0.09 to 0.56. These values are less than 0.16 in oil families 1 to 3, while in oil family 4 it reaches 0.56 indicating the higher maturity of this oil family. The thermal maturity of the oil families is shown in the diagram of $C_{29}\alpha\alpha\alpha20S/(20S + 20R)$ versus Ts/ (Ts + Tm) ratio and $C_{29}\alpha\alpha\alpha20S/(20S + 20R)$ versus C_{27} Dia/ (Dia + Reg) (Fig. 10). As is seen, the thermal maturity of the
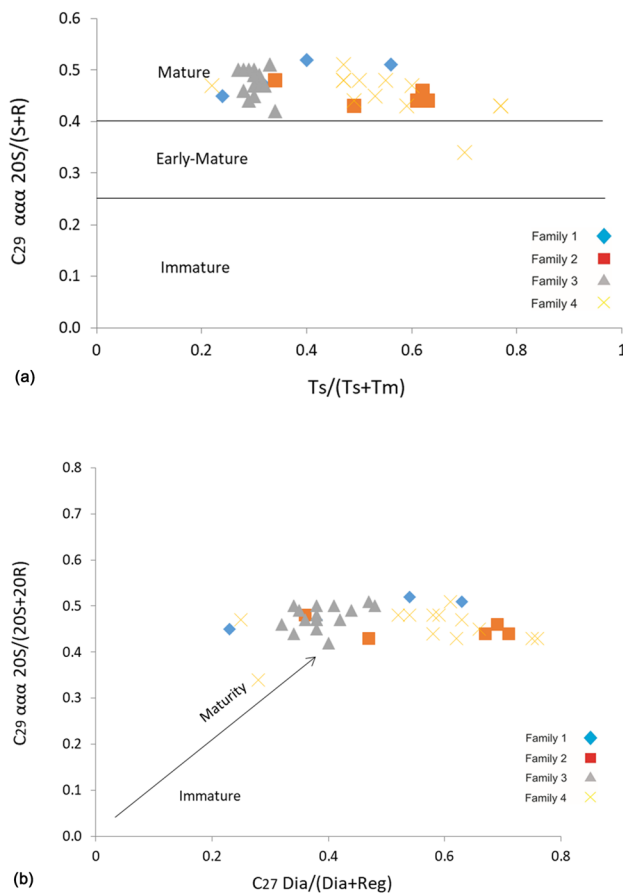
(a)

(b)

Fig. 10 Steranes and trisnorhopane indicate thermally mature source rock of oil families. **A** $C_{29}\alpha\alpha\alpha20S/(20S+20R)$ versus $Ts/(Ts+Tm)$ **B** $C_{29}\alpha\alpha\alpha20S/(20S+20R)$ versus C_{27} Dia/(Dia+Resg)
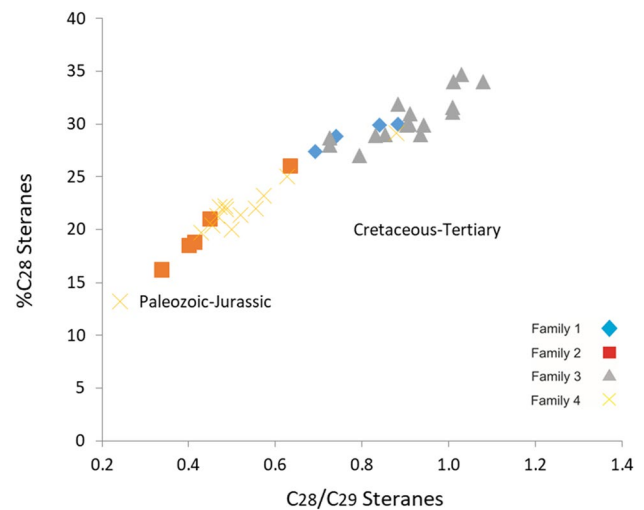

Fig. 11 Estimating the source rocks age of oil families by C_{28}/C_{29} Steranes versus %C_{28} Steranes diagram. Oil family 2 is sourced from the Paleozoic-Jurassic source rocks, while other families belong to the Cretaceous-Tertiary sources

oil families 2 and 4 is older than the other two oil families and is related to the Triassic to Jurassic sediments. The origin of oil family 1 and 3 oils is also estimated as Cretaceous sediments (Table 3). In addition, oil family 3, in the eastern Persian Gulf fields, has the youngest origin among the studied samples. The age of the source rock of oil family 3 is estimated as middle Cretaceous sediments (Fig. 11).

Tectonics activities and oil migration

The age of the possible source rocks of oil families 1 and 3 are estimated as Middle (Upper) Cretaceous Formations. These successions including the Kazhdumi Formation along with the Khatiyah, Ahmadi and Madoud members of the Sarvak Formation. The origin of oil family 2, the Jurassic and older sediments, has also been identified. The possible source rocks of this oil family are the Shale sediments of the Dashtak and Neyriz Formations. The two cases of the discrepancy in the origin of the oil families investigated are as follows: (1) lack of cohesion and integrated deposition of the seal and evaporate Hith Formation in the Persian Gulf and (2) presence of structural features such as a vertical fault and transport of the hydrocarbon by them. During the Tithonian in the Upper Jurassic, the thick anhydrite Hith Formation has been spread in the Persian Gulf region (Sharland et al. 2001; Konyuhov and Maleki 2006). Accordingly, this case is rejected. Therefore, to understand the reason for the similarity of the source of oil families 2 and 4, it is necessary to review the tectonic conditions and structural characteristics of the region. One of the influential factors in petroleum systems is the tectonic characteristics of the sedimentary basin (Ehsan et al. 2021). In the study area, the compressive

oil families falls in the category of mature oils (Fig. 10). In addition, it is found that the thermal maturity of oil family 3 belonging to the east of the Persian Gulf was less than the other three oil families, oil family 2 along with oil family 4, that produce from the Jurassic and older source rocks have the highest thermal maturity (Table 3). This study shows that the samples whose thermal maturity has been detected beyond the oil generation window belong to oil families 2 and 4 located in the center of the Persian Gulf and have different origins from the other samples.

Source rock's age

The source rock's age is estimated using the C_{28} and C_{29} regular steranes. The ratio of C_{28}/C_{29} steranes to the age of the source rock is inversely related. The high value of this ratio in the composition of crude oil indicates the younger source rock and vice versa (Grantham and Wakefield 1988). In the C_{28}/C_{29} Steranes versus the %C_{28} Steranes diagram, the oil families of the Sarvak Formation reservoirs can be distinguished based on the source rock's age. The origin of

strength caused by the collision of the Arabian shield and the Iranian plate has created two folds set in this basin. (1) A set of folds with a high slope and a north–south trend, (2) A set of folds with a northwest-southeast trend along with the sinistral strike-slip fault (Stern 1985). In general, the Phanerozoic sequences in the north of the Arabian Shield are affected mainly by the North–South folds and have large anticlines and narrow synclines (Beydoun 1991). The main structure of the Persian Gulf basin is steep-slope folds with a 7° to the northwest and folds with a lower slope of about 3° to the southeast. The asymmetry of the folds is attributed to the thrust faults with the northwest trend (Ziegler 2001). Also, the north–south trending structures with regular intervals have been formed in the eastern part of the Arabian shield (e.g. the Qatar arch, Ghawar, Burgan, and Suman) due to the east–west compressive strength (Al-Husseini 2000). The dominant tectonic structures in the west and northwest regions of the Persian Gulf basin are the same northwest-southeast trend folds. On the other hand, in the center of the Persian Gulf, where the samples of oil families 2 and 4 were collected, the giant salt domes are effective structures. In the Proterozoic, the evaporative anhydrite/gypsum and salt deposits called the Hormuz series covered the bedrock of the Tethys Ocean sedimentary basin. Afterward, the increase in Paleozoic carbonate sediments and the increase in lithostatic pressure, as well as the activity of the basement rocks on the Gondwana margin following the subduction of the Tethys oceanic crust in the Jurassic and before the closure of the new Tethys in the Lower Cretaceous, had caused the diapirism and salt uplift resulting in giant salt domes (Talbot and Alavi 1996). Observations indicate the presence of these salt diapirs in areas of the Persian Gulf, the Sea of

Oman, and the Zagros frontal basin, but they are absent in the north–south Arabian arches (Memarzia 2004) (Fig. 12). Using the results of seismic and field studies, Sherkati and Letouzey (2004) found the relationship between salt domes and vertical faults in the center of the Persian Gulf. The salt domes of the center of the Persian Gulf have created huge anticlines such that these anticlines have created large vertical faults. Also, these normal faults have created small synclines (Hassanzadeh et al. 2018) (Fig. 13). 3D seismic data were acquired in the field location. The survey covered a total area of approximately 1050 km². The quality of 3D post-stack migration data is reasonably good and faulted graben structures over the Reshadat field can be clearly seen. By studying the seismic profiles of the Lavan province, it turns out that the huge vertical faults range from the Upper Triassic successions to the Santonian Ilam Formation (Fig. 13). It can be concluded that family 2 oils are produced from the Jurassic source rocks. They crossed the anhydrite Hith barrier by the faults in this region and were finally trapped in the Sarvak reservoir. The noteworthy point is that according to the available evidence, it was concluded that the hypothesis of hydrocarbon migration by faults in the central oilfields of the Persian Gulf is more probable, but the rest of the hypotheses cannot be definitively rejected with the available information.

Conclusions

The current study employs a complete set of geochemical from the Iranian part of Persian Gulf to draw regional interpretation of geochemical data. For this purpose, a
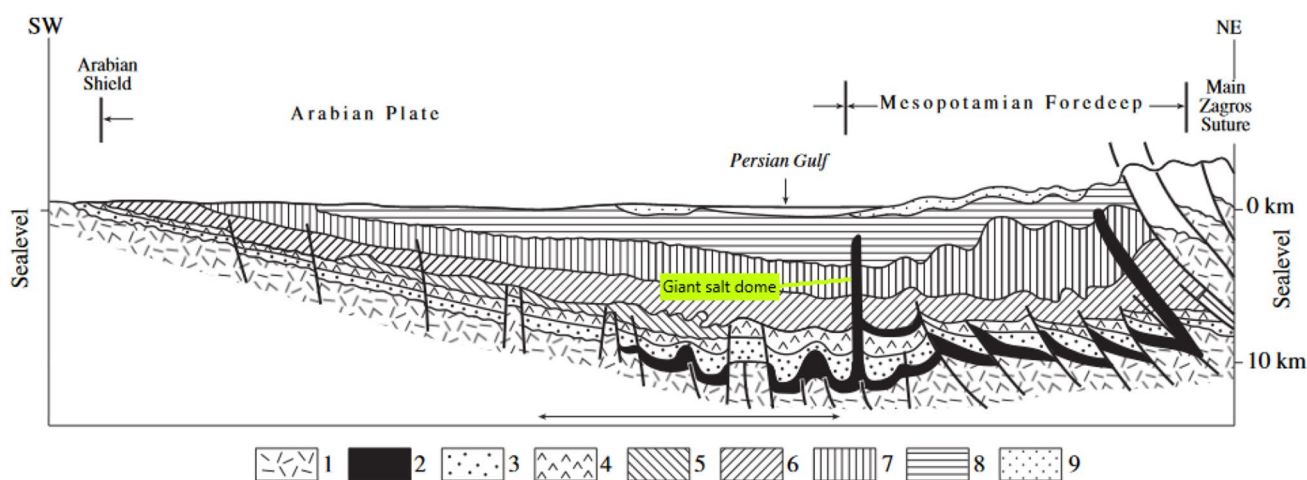

Fig. 12 The giant salt dome is observed in the SW-NE stratigraphic section of the Persian Gulf region. Apart from basement faults, many normal faults occurred in the study area due to the upwards movements of the salt diapir. 1: Basement rock, 2: Hormuz salt, 3: Sandstone, 4: Anhydrite/gypsum, 5: Dolomite, 6: Dolomitic limestone, 7: Limestone, 8: Marl-limestone, 9: Conglomerate (modified from Edgell 1996)
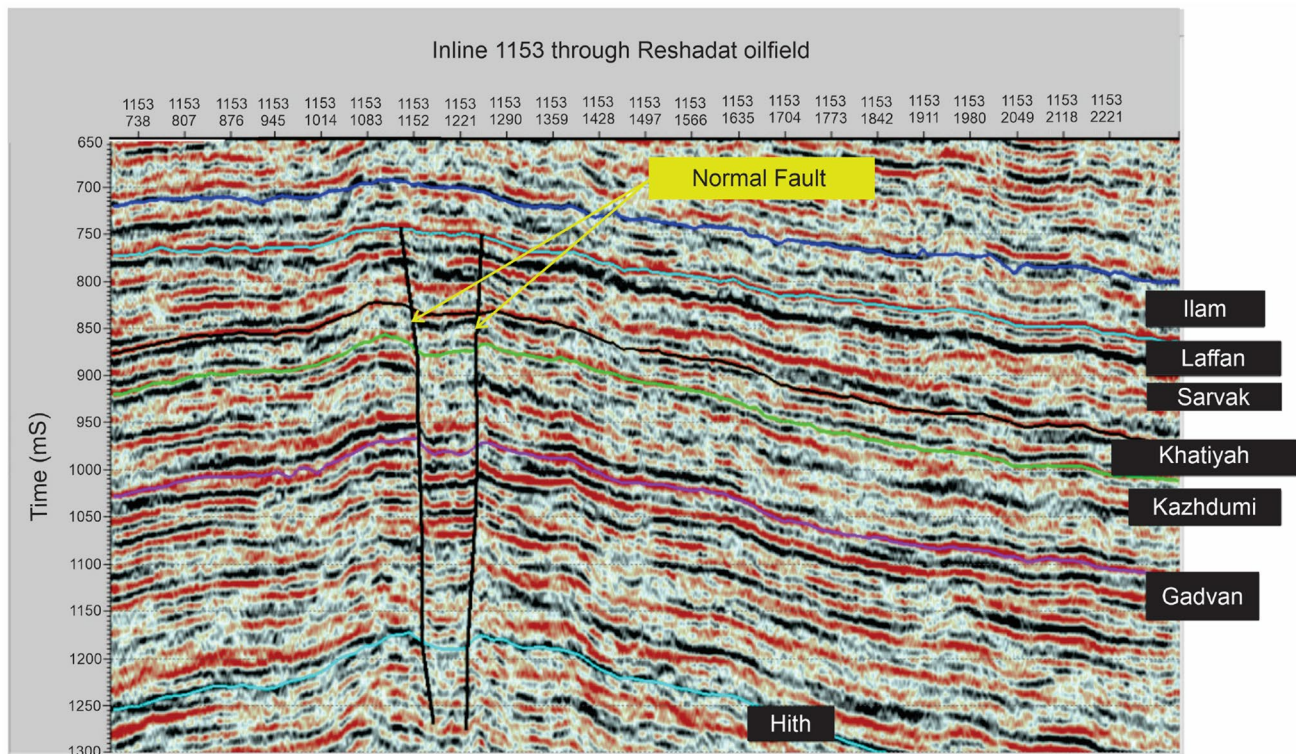
Fig. 13 The seismic profile representing two normal faults affecting the Sarvak reservoir. The Jurassic source rocks crossed the anhydritic Hith barrier by faults existing in the study area and causing its migration to the Sarvak reservoir. The unit of length on the horizontal axis is meter

total of 41 oil samples from 10 oilfields were collected and assessed based on gas chromatography (GC), gas chromatography–mass spectrometry (GC–MS) and stable carbon isotope analysis. Considering the results of this study, the followings conclusions are drawn.

- The oil samples of the Sarvak reservoirs from ten oilfields in the western, central and eastern parts of the Persian Gulf were evaluated using hierarchical cluster analysis (HCA), star diagrams and the Galimov isotopic diagrams. The oils were divided into four families based on characteristics of their origin.
- The Sarvak reservoirs oils in the western Persian Gulf (oil family 1) have a Cretaceous source rock formed in a shaly sedimentary environment with dysoxic conditions, normal salinity, no stratification and medium maturity in the oil generation window.
- The Sarvak reservoirs oils in the central Persian Gulf (oil families 2 and 4) have the Jurassic and earlier source rocks formed in carbonate-marl sedimentary environments with anoxic to dysoxic conditions, low salinity and stratification and high thermal maturity.
- The Cretaceous rocks deposited in a carbonate-marl environment with anoxic conditions, low salinity and stratification and low thermal maturity charge the Sar-

vak reservoirs in the eastern Persian Gulf basin (oil family 3)
- It was found that oil families 2 and 4 have more mature and older oils than families 1 and 3.
- The geochemical differences in the oils are attributed to the presence of normal vertical faults.
- The migration of hydrocarbons from the Surmeh oil reservoirs at a depth of about 2400 m to the Sarvak oil reservoirs at a depth of about 1000 m has occurred through these faults.

Appendix A. Biomarker Parameters

HCA was plotted using 22 biomarker parameters. The biomarker ratios include C_{19}/C_{23} Tricyclic Terpane, C_{22}/C_{21} Tricyclic Terpane, C_{22}/C_{24} Tricyclic Terpane, C_{24}/C_{23} Tricyclic Terpane, C_{26}/C_{25} Tricyclic Terpane, C_{24} Tetracyclic Terpane/C_{23} Tricyclic Terpane, C_{24} Tetracyclic Terpane/C_{26} Tricyclic Terpane, C_{23} Tricyclic Terpane /C_{30} Hopane, C_{29}/C_{30} Hopane, C_{30} DiaH/C_{30} Hopane, Olenane/C_{30} Hopane, C_{30} Trisnorhopane /C_{30} Hopane, Gammacerane/C_{31} homohopane, C_{35} Homohopane Index, C_{35}/C_{34} homohopane 22S, %$C_{27}\alpha\alpha\alpha$ 20R, %$C_{28}\alpha\alpha\alpha$ 20R, %$C_{29}\alpha\alpha\alpha$ 20R, C_{27} Diasteranes/(Diasteranes + Regular Steranes), ($C_{21} + C_{22}$)/

$(C_{27} + C_{28} + C_{29})$ Sterane, C_{29}/C_{27} αββ Sterane Ratio, Dibenzothiophene /Phenanthrene.

Declarations

Conflict of interest The authors declare that they have no known competing financial interests or personal relationships that could have appeared to influence the work reported in this paper.

Ethical approval This material is the authors' own original work, which has not been previously published elsewhere. The paper is not currently being considered for publication elsewhere. The paper reflects the authors' own research and analysis in a truthful and complete manner. The publication of this manuscript does not engage in or participate in any form of malicious harm to another person or animal.

References

Al-Husseini MI (2000) Origin of the Arabian plate structures: Amar Collision and Najd Rift. GeoArabia 5:527–542. https://doi.org/10.2113/geoarabia0504527

Alizadeh B, Alipour M, Chehrazi A, Mirzaie S (2017) Chemometric classification and geochemistry of oils in the Iranian sector of the southern Persian Gulf Basin. Org Geochem 111:67–81. https://doi.org/10.1016/j.orggeochem.2017.05.006

Allen MB, Armstrong A (2008) Arabia-Eurasia collision and the forcing of mid-Cenozoic global cooling. Palaeogeogr Palaeoclimatol Palaeoecol 265:52–58

Alsharhan AS (2014) Petroleum systems in the Middle East. Geol Soc London Spl Publ 392:361–408. https://doi.org/10.1144/SP392.19

Aram Z, Arian M (2016) Active tectonics of the Gharasu river basin in Zagros Iran investigated by calculation of geomorphic indices and group decision using analytic hierarchy process (AHP) software. Episodes J Int Geosci. https://doi.org/10.18814/epiiugs/2016/v39i1/89235

Arian M (2012) Clustering of diapiric provinces in the Central Iran Basin. Carbonates Evaporites 27:9–18. https://doi.org/10.1007/s13146-011-0079-9

Arian M (2015) Seismotectonic-Geologic Hazards Zoning of Iran. Earth Sciences Research Journal 19: 7–13. https://doi.org/10.15446/esrj.v19n1.40664

Arian M, Aram Z (2014) Relative tectonic activity classification in the Kermanshah area, Western Iran. Solid Earth 5:1277–1291. https://doi.org/10.5194/se-5-1277-2014

Arian M, Bagha N, Khavari R, Noroozpour H (2012) Seismic sources and neo-tectonics of Tehran Area (North Iran). Indian J Sci Technol 5:2379–2383. https://doi.org/10.17485/ijst/2012/v5i3.21

Baniasad A, Kassaei M, Mirshahani M, Ghorbani B, Akbarpour S, Memariani M, Beiranvand B (2016) 3D petroleum systems modeling in the Persian Gulf & Oman sea. Unpublished report of the Research Institute of Petroleum Industry (RIPI)

Baniasad A, Littke R, Froidl F, Grohmann S, Soleimany B (2021) Quantitative hydrocarbon generation and charge risk assessment in the NW Persian Gulf: a 3D basin modeling approach. Marine Petrol Geol. https://doi.org/10.1016/j.marpetgeo.2021.104900

Beach F, Peakman TM, Abbott GD, Sleeman R, Maxwell JR (1989) Laboratory thermal alteration of triaromatic steroid hydrocarbons. Org Geochem 14:109–111

Beaumont C, Boutlier R, Mackenzie AS, Rullkötter J (1985) Isomerization and aromatization of hydrocarbons and the paleothermometry and burial history of Alberta Foreland Basin. Am Asso Petrol Geol Bull 69:546–566

Beydoun ZR (1991) Arabian plate hydrocarbon geology and potential—a plate tectonic approach. American Association of Petroleum Geologists https://doi.org/10.1306/St33533

Bordenave ML, Hegre JA (2010) Current distribution of oil and gas fields in the Zagros Fold Belt of Iran and contiguous offshore as the results of the petroleum system. In: Leturmy P, Robin C (Eds) Tectonic and stratygraphic evolution of Zagros and Makran during the Mesozoic-Cenozoic Geological Society Special Publication 330, London https://doi.org/10.1144/SP330.14

Didyk BM, Simoneit BRT, Brassell SC, Eglinton G (1978) Organic geochemical indicators of palaeoenvironmental conditions of sedimentation. Nature 272:216–222. https://doi.org/10.1038/272216a0

Edgell HS (1996) Salt tectonism in the Persian Gulf Basin. Geol Soc Spec Pub 100:129–151. https://doi.org/10.1144/GSL.SP.1996.100.01.10

Ehsan M, Gu H, Ali A, Akhtar MM, Abbasi SS, Faisal Miraj MA, Shah M (2021) An integrated approach to evaluate the unconventional hydrocarbon generation potential of the Lower Goru Formation (Cretaceous) in Southern Lower Indus basin, Pakistan. J Earth Syst Sci 130:90. https://doi.org/10.1007/s12040-021-01584-4

Ehsani J, Arian M (2015) Quantitative analysis of relative tectonic activity in the Jarahi–Hendijan Basin Area, Zagros Iran. Geosci J 19:1–15. https://doi.org/10.1007/s12303-015-0016-3

El-Naggar ZR, Al-Rifai IA (1972) Stratigraphy and Microfacies of Type Magwa Formation of Kuwait, Arabia; Part I: Rumaila Limestone Member. AAPG Bull 56:10

Galimov EM (1973) Geochemistry of carbon and its applications in oil and gas exploration. Nedra Press, Moscow

Ghanadian M, Faghih A, Abdollahie Fard I, Grasemann B, Soleimany B, Maleki M (2017) Tectonic constraints for hydrocarbon targets in the Dezful embayment, Zagros fold and thrust belt, SW Iran. J Petrol Sci Eng 157:1220–1228. https://doi.org/10.1016/j.petrol.2017.02.004

Ghazban F (2007) Petroleum geology of the Persian Gulf Joint publication. Tehran University Press and National Iranian Oil Company

Grantham PJ, Wakefield LL (1988) Variations in the sterane carbon number distribution of marine source rock derived crude oils through geological time. Org Geochem 12:61–73. https://doi.org/10.1016/0146-6380(88)90115-5

Hassanzadeh P, Rabbani AR, Hezarkhani A, Khajooie S (2018) Assessing lateral continuity within the yammama reservoir in the

Foroozan oilfield, offshore Iran: an integrated study. Acta Geol Sin 92:2405–2415. https://doi.org/10.1111/1755-6724.13736

Hessami K, Nilforoushan F, Talbot CJ (2006) Active deformation within the Zagros Mountains deduced from GPS measurements. J Geol Soc 163:143–148. https://doi.org/10.1144/0016-764905-031

Hughes WB, Holba AG, Dzou LIP (1995) The ratios of dibenzothiophene to phenanthrene and pristane to phytane as indicators of depositional environment and lithology of petroleum source rocks. Geochim Cosmochim Acta 59:3581–3598. https://doi.org/10.1016/0016-7037(95)00225-O

James GA, Wynd JG (1965) Stratigraphic Nomenclature of Iranian Oil Consortium Agreement Area. AAPG Bull 49:2182–2245

Kadkhodaie A, Kadkhodaie R (2022a) Reservoir characterization of tight gas sandstones: exploration and development. Elsevier Book, 265 https://doi.org/10.1016/C2020-0-02860-4

Kadkhodaie A, Kadkhodaie R (2022) Chapter 1 - Tight sandstones: overview, distribution, and global significance. In: Kadkhodaie A, Kadkhodaie R (eds) Reservoir characterization of tight gas sandstones: exploration and development. Elsevier, New York, pp 1–22. https://doi.org/10.1016/B978-0-323-90180-2.00010-4

Khalil Khan H, Ehsan M, Ali A, Amer MA, Aziz H, Khan A, Bashir Y, Abu-Alam T, Abioui M (2022) Source rock geochemical assessment and estimation of TOC using well logs and geochemical data of Talhar Shale, Southern Indus Basin, Pakistan. Front Earth Sci 10:969936. https://doi.org/10.3389/feart.2022.969936

Khavari R, Arian M, Ghorashi M (2009) Neotectonics of the South Central Alborz Drainage Basin, in NW Tehran, N Iran. J Appl Sci 9:4115–4126. https://doi.org/10.3923/jas.2009.4115.4126

Konyuhov AI, Maleki B (2006) The Persian Gulf Basin: geological history, sedimentary formations, and petroleum potential. Lithol Miner Resour 41:344–361. https://doi.org/10.1134/S0024490206040055

Mansouri E, Feizi F, Jafari Rad A, Arian M (2017) A comparative analysis of index overlay and topsis (based on ahp weight) for Iron Skarn Mineral prospectivity mapping, a case study in Sarvian Area, Markazi Province, Iran. Bull Miner Res Explor 155:147–160. https://doi.org/10.19111/bulletinofmre.305201

Mansouri E, Feizi F, Jafari Rad A, Arian M (2018) Remote-sensing data processing with the multivariate regression analysis method for iron mineral resource potential mapping: a case study in the Sarvian area, central Iran. Solid Earth 9:373–384. https://doi.org/10.5194/se-9-373-2018

Mashhadi ZS, Rabbani AR (2015) Organic geochemistry of crude oils and Cretaceous source rocks in the Iranian sector of the Persian Gulf: an oil–oil and oil–source rock correlation study. Int J Coal Geol 146:118–144

McKirdy DM, Kantsler AJ, Emmett JK, Aldridge AK (1984) Hydrocarbon genesis and organic facies in Cambrian carbonates of the Eastern Officer Basin, South Australia. In: Petroleum Geochemistry and Source Rock Potential of Carbonate Rocks (J. G. Palacas, ed.) American Association of Petroleum Geologists Geology, Tulsa, OK, pp 13–31.

Memarzia A (2004) The role of interpretation of reflective seismic data in the exploration of hydrocarbon resources. Iranian Offshore Oil Company, p 256

Mohammadrezaei H, Alavi SA, Cardozo N, Ghassemi MR (2020) Deciphering the relationship between basement faulting and two-phase folding in the Hendijan anticline, northwest Persian Gulf, Iran. Marine Petrol Geol 122:104626. https://doi.org/10.1016/j.marpetgeo.2020.104626

Motiei H (1993) Geology of Iran. The stratigraphy of Zagros. Geological survey of Iran

Nabilou M, Arian M, Afzal P, Adib A, Kazemi A (2018) Determination of relationship between basement faults and alteration zones in Bafq-Esfordi region, central Iran. Episodes J Int Geosci 41:143–159. https://doi.org/10.18814/epiiugs/2018/018013

Nouri R, Arian M (2017) Multifractal modeling of the gold mineralization in the Takab area (NW Iran). Arab J Geosci 10:105. https://doi.org/10.1007/s12517-017-2923-2

Nouri R, Jafari MR, Arian M, Feizi F, Afzal P (2013) Prospection for copper mineralization with contribution of remote sensing, geochemical and mineralographical data in abhar 1:100,000 Sheet, NW Iran. Arch Min Sci 58:1071–1084. https://doi.org/10.2478/amsc-2013-0074

Ourisson G, Rohmer M, Poralla K (1987) Prokaryotic hopanoids and other polyterpenoid sterol surrogates. Annu Rev Microbiol 41:301–333

Owen RMS, Nasr SN (1958) Stratigraphy of the Kuwait-Basra area. In: Weeks LG (ed) Habitat of oil, AAPG, Memoir, vol 1, pp 1252–1278

Peters JM, Filbrandt JB, Grotzinger JP, Newall MJ, Shuster M, Al-Siyabi HA (2003) Surface-piercing salt domes of interior North Oman, and their significance for the Ara carbonate 'stringer' hydrocarbon play. GeoArabia 8:231–270. https://doi.org/10.2113/geoarabia0802231

Peters KE, Moldowan JM (1993) The Biomarker guide: interpreting molecular fossils in petroleum and ancient sediments. Englewood Cliffs, Prentice-Hall, New Jersey, p 363

Peters KE, Moldowan JM, Sundararaman P (1990) Effects of hydrous pyrolysis on biomarker thermal maturity parameters: Monterey Phosphatic and Siliceous Members. Org Geochem 15:249–265

Peters KE, Walters CC, Moldowan JM (2005) The Biomarker Guide. Biomarkers and Isotopes in Petroleum Exploration and Earth History 2nd (ed). Cambridge University Press, Cambridge

Pollastro RM (2003) Total petroleum systems of the Paleozoic and Jurassic, Greater Ghawar Uplift and adjoining provinces of Central Saudi Arabia and Northern Arabia-Persian Gulf. United States Geological Survey Bulletin, 2202-H. https://doi.org/10.3133/b2202H

Powell TG, Mckirdy DM (1973) Relationship between ratio of pristane to phytane, crude oil composition and geological environment in Australia. Nature 243:37–39. https://doi.org/10.1038/physci243037a0

Rabbani AR (2013) Petroleum geology and geochemistry of the Persian Gulf. Tafresh University, Tafresh

Rabbani AR, Kotarba MJ, Baniasad AR, Hosseiny E, Wieclaw D (2014) Geochemical characteristics and genetic types of the crude oils from the Iranian sector of the Persian Gulf. Org Geochem 70:29–43. https://doi.org/10.1016/j.orggeochem.2014.02.010

Razaghian G, Beitollahi A, Pourkermani M, Arian M (2018) Determining seismotectonic provinces based on seismicity coefficients in Iran. J Geodyn 119:29–46. https://doi.org/10.1016/j.jog.2018.05.007

Safaei-Farouji M, Kamali M, Hakimi MH (2022) Hydrocarbon source rocks in Kazhdumi and Pabdeh formations-a quick outlook in Gachsaran oilfield, SW Iran. J Petrol Explor Prod Technol 12:1489–1507. https://doi.org/10.1007/s13202-021-01413-w

Seifert WK, Moldowan JM (1978) Applications of steranes, terpanes and monoaromatics to the maturation, migration and source of crude oils. Geochim Cosmochim Acta 42:77–95. https://doi.org/10.1016/0016-7037(78)90219-3

Seifert WK, Moldowan JM (1986) Use of biological markers in petroleum exploration. In: Johns RB (ed) Methods in Geochemistry and Geophysics, vol 24. Elsevier, Amsterdam, pp 261–290

Sepehr M, Cosgrove JW (2004) The structural framework of the Zagros Fold-Thrust Belt. Iran Marine and Petroleum Geology 21:829–843. https://doi.org/10.1016/j.marpetgeo.2003.07.006

Sharland PR, Archer R, Casey DM, Davies RB, Hall SH, Heward AP, Simmons MD (2001) Sequence stratigraphy of the Arabian Plate. GeoArabia 2:101–130. https://doi.org/10.2113/geoarabia1204101

Sherkati S, Letouzey J (2004) Variation of structural style and basin evolution in the central Zagros (Izeh zone and Dezful Embayment). Iran Marine Petrol Geol 21:535–554. https://doi.org/10.1016/j.marpetgeo.2004.01.007

Sinninghe Damsté JS, de Leeuw JW (1995) Biomarkers or not biomarkers: a new hypothesis for the origin of pristane involving derivation from methyltrimethyltridecylchromans (MTTCs) formed during diagenesis from chlorophyll and alkylphenols. Organic Geochemistry 23:1085–1093.

Song J, Littke R, Weniger P (2017) Organic geochemistry of the Lower Toarcian Posidonia Shale in NW Europe. Org Geochem 106:76–92. https://doi.org/10.1016/j.orggeochem.2016.10.014

Stern RJ (1985) The Najd fault system, Saudi Arabia and Egypt: a late Precambrian rift-related transform system. Tectonics 4:497–511. https://doi.org/10.1029/TC004i005p00497

Taesiri V, Pourkermani M, Sorbi A, Almasian M, Arian M (2020) Morphotectonics of Alborz Province (Iran): a case study using GIS method. Geotectonics 54:691–704. https://doi.org/10.1134/S001685212005009X

Talbot CJ, Alavi M (1996) The past of a future syntaxis across the Zagros. Geol Soc London 100:89–109. https://doi.org/10.1144/GSL.SP.1996.100.01.08

Ward JH (1963) Hierarchical grouping to optimize an objective function. J Am Stat Assoc 58:236

Ziegler MA (2001) Late permian to holocene paleofacies evolution of the Arabian plate and its hydrocarbon occurrences. GeoArabia 6:445–504. https://doi.org/10.2113/geoarabia0603445

Publisher's Note Springer Nature remains neutral with regard to jurisdictional claims in published maps and institutional affiliations.